Catal Lett (2009) 127:277–284
DOI 10.1007/s10562-008-9672-5

Catalytic Activity of Y Zeolite Supported CeO_2 Catalysts for Deep Oxidation of 1, 2-Dichloroethane (DCE)

Jianmin Zhou · Lan Zhao · Qinqin Huang · Renxian Zhou · Xiaokun Li

Received: 7 July 2008 / Accepted: 14 September 2008 / Published online: 7 October 2008

Abstract Three Y zeolites supported CeO_2 catalysts (CeO_2/USY, CeO_2/HY, CeO_2/SSY) were prepared and used for deep oxidation of 1,2-dichloroethane (DCE) in low concentration (about 1,000 ppm). The catalysts were characterized by XRD, N_2 adsorption/desorption and H_2-TPR. The results showed that the catalytic activity of the supported CeO_2 catalysts was much higher than that of Y zeolites, in particular, CeO_2/USY exhibited the highest activity, $T_{98\%}$ values of DCE was about 270 °C. And the catalytic activity was strongly related to the interaction between CeO_2 and Y zeolites.

Keywords CeO_2/USY · Catalytic oxidation · DCE

1 Introduction

Chlorinated volatile organic compounds (CVOCs), such as dichloromethane (DCM), 1,2-dichloroethane (DCE), and trichloroethylene (TCE), are a wide ranging class of solvents commonly found in industrial waste streams and constitute a major source of air and groundwater pollution [1]. The increasing amounts of CVOCs released in the environment, together with their suspected toxicity and carcinogenic properties, have prompted researchers world-wide to find clean effective methods of destruction. The abatement of CVOCs by catalytic combustion has been widely utilized in several technical processes [2]. Moreover, catalytic oxidation appears to be more efficient for the abatement of low concentrations of contaminant (<1,000 ppm), which cannot be thermally combusted without additional fuel [3].

Most reported studies of the catalysts for CVOC catalytic combustion have focused on three types of catalysts based on noble metals, transition metals, and zeolites. Noble metal catalysts such as Pt, Pd, Rh, and Ru are very active for the destruction of CVOCs, but the halide (HCl and Cl_2 produced from the decomposition of CVOCs) deactivation is still avoidless [4, 5]. Traditionally, supported transition metal oxides have been proposed as the potential substitutes for the noble metal-based catalysts [6]. Transition metal oxides are in general less catalytic active than noble metals for the destruction of CVOCs, but they can resist the deactivation by poisoning largely [7]. Among these catalysts, chromium-based catalysts have exhibited the highest activity for CVOCs destruction [8–10]. Nevertheless, the uses of chromium-based catalysts are restricted, owing to the formation of the extremely toxic residues (such as chromium oxychloride) at low temperature [11]. Consequently, there is interest in developing catalysts that are less expensive and more robust than the materials presently in use. For these reasons, there are strong interests to develop alternative efficient catalysts for CVOC oxidation.

Zeolites, like Y, X, BETA, ZSM-5, and MCM-41 have traditionally received great interest because of their optimum performances as solid acid catalysts in refining and petrochemical processes [12, 13] and as adsorbents in many separation and purification processes [14]. In the last few years, a few investigations reported on the literature have also proved that zeolites with the strong acid sites play a key role in controlling the decomposition of chlorinated compounds, but less consideration has been given to their applicability as potential catalysts for the

J. Zhou · L. Zhao · X. Li
Wenzhou Medicine College, Wenzhou 325035, People's Republic of China

Q. Huang · R. Zhou (✉)
Institute of Catalysis, Zhejiang University, Hangzhou 310028, People's Republic of China
e-mail: zhourenxian@zju.edu.cn

decomposition of CVOCs [15–20], due to have lower catalytic activity of deep oxidation, and they easily produce coke deposition, which results in the catalyst deactivation.

The rare-earth elements have been used widely in the environmental catalysts. Especially cerium oxide has much more attracted attention in three-way catalysts and been used an effective promoter or supporting material based on its high oxygen-storage capacity (OSC) and facile redox cycle of Ce^{4+}/Ce^{3+} [21–23]. Supported CeO_2 and CeO_2 based mixed oxides are also cheap, environmentally friendly and efficient catalysts for the catalytic destruction of non-chlorinated VOCs [24–27], such as methane, CO, methanol, and propane. They can be also used in the wet oxidation processes of the organic compounds, such as the treatment of the industrial waste-waters and the removal of total organic carbon from polluted waters [28–33]. Recently, the supported CeO_2 and CeO_2-based mixed oxides have attracted considerable attention for the decomposition of CVOCs (DCE, TCE, DCM) [35–39]. These studies indicate that $Ce_xZr_{1-x}O_2$ mixed oxides exhibit better redox and acidic properties than pure CeO_2, and $Ce_{0.5}Zr_{0.5}O_2$ showed the best performance.

In the process of CVOCs decomposition, the dehydrochlorination occurs usually at lower temperature, and then intermediates are further oxidized [2, 18, 34, 40]. So, the acidic sites in the catalysts and their oxidation ability play a very important role to the catalytic performance. In this article, our purpose is to examine the catalytic oxidation performance of Y zeolite supported CeO_2 catalysts for the catalytic oxidation of DCE in low concentration and studied the relationship between the catalytic activity and properties of these CeO_2/Y catalysts.

2 Experimental

2.1 Catalysts Preparation

NH_4Y, USY, and SSY were supplied by HUAHUA Corp. HY was obtained by calcination of NH_4Y zeolite at 550 °C for 2 h in air. CeO_2 was prepared by thermal decomposition of $Ce(NO_3)_3 \cdot 6H_2O$ (AR, 98.0%) at 550 °C for 2 h in air.

Three supported catalysts (CeO_2/USY, CeO_2/HY, CeO_2/SSY with weight ratio of 1/8) were prepared by impregnation method. Dried at 100 °C for 2 h, and then calcined at 350 °C for 0.5 h and 550 °C for 2 h in air.

2.2 Catalysts Characterization

2.2.1 X-Ray Powder Diffraction (XRD)

The phase composition of the various samples was determined by means of X-ray powder diffraction (XRD), using a RigakuD/max-3BX. The operating parameters were as follow: monochromatic Cu Kα radiation, Ni filter, 40 mA, 40 kV, between 2θ values 3° and 70°.

2.2.2 Nitrogen Adsorption/Desorption

The surface areas of the samples were determined by nitrogen adsorption/desorption at liquid nitrogen temperature using a Coulter OMNISORP-100 apparatus. The samples were degassed under vacuum for 3 h at 200 °C before the measurements. Specific total surface area was calculated using the Brunauer–Emmett–Teller (BET) equation.

2.2.3 Temperature-Programmed Reduction (H_2-TPR)

Temperature-programmed reduction (H_2-TPR) was carried out in a flow system to observe reducibility of the supported catalysts. Prior to H_2-TPR measurement, 100 mg catalyst was pre-treated at 300 °C for 0.5 h in air. The reductive gas was a mixture of 5 vol.% H_2 in Ar (40 mL/min), which was purified using deoxidizer and silica gel. Temperature of the sample was programmed to rise at a constant rate of 15 °C/min. The amount of hydrogen uptakes during the reduction was measured by a thermal conductivity detector (TCD), and the effluent H_2O formed during H_2-TPR was absorbed with a 5 Å molecular sieve. The hydrogen uptakes were quantified using CuO as a standard.

2.2.4 NH_3-TPD

Temperature-programmed desorption (TPD) of NH_3 was carried out in a flow system to observe acidic properties of the catalysts. Prior to NH_3-TPD experiments, the samples (100 mg) were first pre-treated in a quartz tube for 0.5 h in an He stream at 500 °C to removal the surface adsorption substance. Then, they were cool down to 100 °C. At 100 °C, keep the samples in a NH_3 flow (20 mL min^{-1}) for 0.5 h. Subsequently, the samples were exposed to a flow of helium for 1 h at 100 °C in order to remove reversibly and physically bound ammonia from the surface. Finally, desorption was carried out from 100 to 600 °C at a heating rate of 10 °C min^{-1}.

2.3 Catalytic Activity Tests

The catalytic activity in the complete oxidation of DCE was measured in a continuous flow micro-reactor system at atmospheric pressure with a quartz tube reactor. 0.3 mL catalyst was placed in the middle of reactor, and the space velocity (GHSV) was 10,000 h^{-1}. The concentration of DCE was about 1,000 ppm, which was prepared by

delivering the liquid DCE by a syringe pump into dry air (dried by silica gel and 5A zeolite), which was metered by a mass flow controller. The gas stream was analyzed with an on-line gas chromatograph equipped with an OV101 column connected to a FID for the detection of organic molecules. Furthermore, MS was used to monitor and confirm the formation of by-products.

3 Results and Discussion

3.1 Catalytic Activity Tests

Table 1 and Fig. 1a show the catalytic activity of CeO_2, USY, HY, SSY, CeO_2/USY, CeO_2/HY, and CeO_2/SSY for the catalytic oxidation of DCE. From Table 1 and Fig. 1a, it can be seen that the catalytic activity of CeO_2, USY, HY, and SSY is low, while the catalytic activity of CeO_2/Y catalysts is evidently increased. $T_{98\%}$ of CeO_2/USY, CeO_2/SSY, and CeO_2/HY is about 90, 10, and 80 °C lower than that of their supports, respectively, The catalytic activity of these supports for the oxidation of DCE decreases in the order: USY > HY > SSY, while the catalytic activity of the loading CeO_2 catalysts decreases in the order: CeO_2/USY, CeO_2/SSY > CeO_2/HY, which indicates that different characteristics of USY, HY, and SSY zeolites would result in different synergies between CeO_2 and Y-type zeolites and catalytic activity for the oxidation of DCE. The modified Y-type zeolites have strong Brønsted acidity and porosity, while CeO_2 has more Lewis sites and good redox property. So these CeO_2/Y materials would take on adsorbent and catalytic properties simultaneously. González-Velasco and coworkers [34] demonstrates that acid sites play a key role in controlling the decomposition of chlorinated compounds over zeolites (SiO_2–Al_2O_3) since they act as effective chemisorption for such compounds. In addition, the porosity of Y-type zeolites is beneficial to the dispersion of CeO_2, which would promote oxidation activity of the CeO_2/Y catalysts. Simultaneously, this would also decrease significantly coke deposition on zeolites surface, which is caused by the strong acidity of zeolites.

The main intermediates and oxidation products (Cl_2, HCl, CH_3Cl, C_2H_3Cl, CH_3CHO, and CH_3COOH) are measured during catalytic destruction of DCE. And infinitesimal $C_2H_2Cl_2$ is also detected. The temperature–concentration relationships of C_2H_3Cl, CH_3CHO, CH_3COOH, $C_2H_2Cl_2$, and CH_3Cl are shown in Fig. 1b–f. The data of maximum concentration and peak temperature are listed in Table 2.

According to the literature [35], the mechanism of the oxidation of DCE is known as follows: The decomposition occurs through by dehydrochlorination into vinyl chloride in the presence of acid sites. This intermediate can be attacked by nucleophilic oxygen species from the catalyst to form chlorinated alkoxide species, which readily decompose to gradually generate acetaldehyde, acetates and CO_x.

Table 1 $T_{50\%}$ and $T_{98\%}$ of DCE for different Y zeolite supports and CeO_2/Y catalysts

Catalysts	CeO_2	USY	HY	SSY	CeO_2/USY	CeO_2/HY	CeO_2/SSY
$T_{50\%}$ (°C)	285	250	275	300	215	280	210
$T_{98\%}$ (°C)	350	360	370	370	270	360	290

Figure 1b shows the temperature–concentration relationship of C_2H_3Cl. From Fig. 1b, it can be seen that the main intermediate is C_2H_3Cl in the oxidation of DCE at low temperature. The peak temperatures at which C_2H_3Cl reaches its maximum concentration are relatively low on CeO_2/USY and CeO_2/SSY, at about 300 and 280 °C, respectively, compared with their supports (about 340 and 360 °C) and CeO_2 (about 320 °C). On CeO_2/USY and CeO_2/SSY, the peak temperature is lower while C_2H_3Cl reaches the maximum concentration. It indicates that there is higher dehydroclorination decomposition activity for DCE destruction on CeO_2/USY and CeO_2/SSY.

Figure 1c, d show the temperature–concentration relationship of CH_3CHO and CH_3COOH. From Fig. 1c, d, it can be seen that the maximum concentrations of CH_3CHO and CH_3COOH are the highest on CeO_2. The maximum concentrations of these two intermediates are higher on CeO_2/Y catalysts than that on their supports, while the peak temperatures at which the maximum concentrations reach are lower. There are two maximum concentrations on CeO_2/USY and CeO_2/SSY. The first peak temperature at which CH_3CHO and CH_3COOH reaches maximum concentrations appears at about 260 °C, and the second one appears at about 370 or 340 °C, respectively. This indicates that the deep oxidative ability of CeO_2, CeO_2/USY, and CeO_2/SSY for DCE is much stronger than other catalysts.

Figure 1e shows the temperature–concentration relationship of infinitesimal by-product $C_2H_2Cl_2$. From Fig. 1e, it can be seen that more $C_2H_2Cl_2$ are produced on CeO_2, CeO_2/USY, and CeO_2/SSY than on other catalysts, which means that there is higher dehydrogenization performance on these catalysts.

Figure 1f shows the temperature–concentration relationship of CH_3Cl. From Fig. 1f it can be seen that when the reacting temperature reaches higher than 350 °C, the quantity of CH_3Cl increases evidently as the temperature increases on all supports and catalysts. At about 420 °C, the maximum concentration of CH_3Cl appears on CeO_2/SSY and CeO_2/USY, about 104 and 64 ppm, respectively. At the opposite, the concentration of CH_3Cl on CeO_2/HY

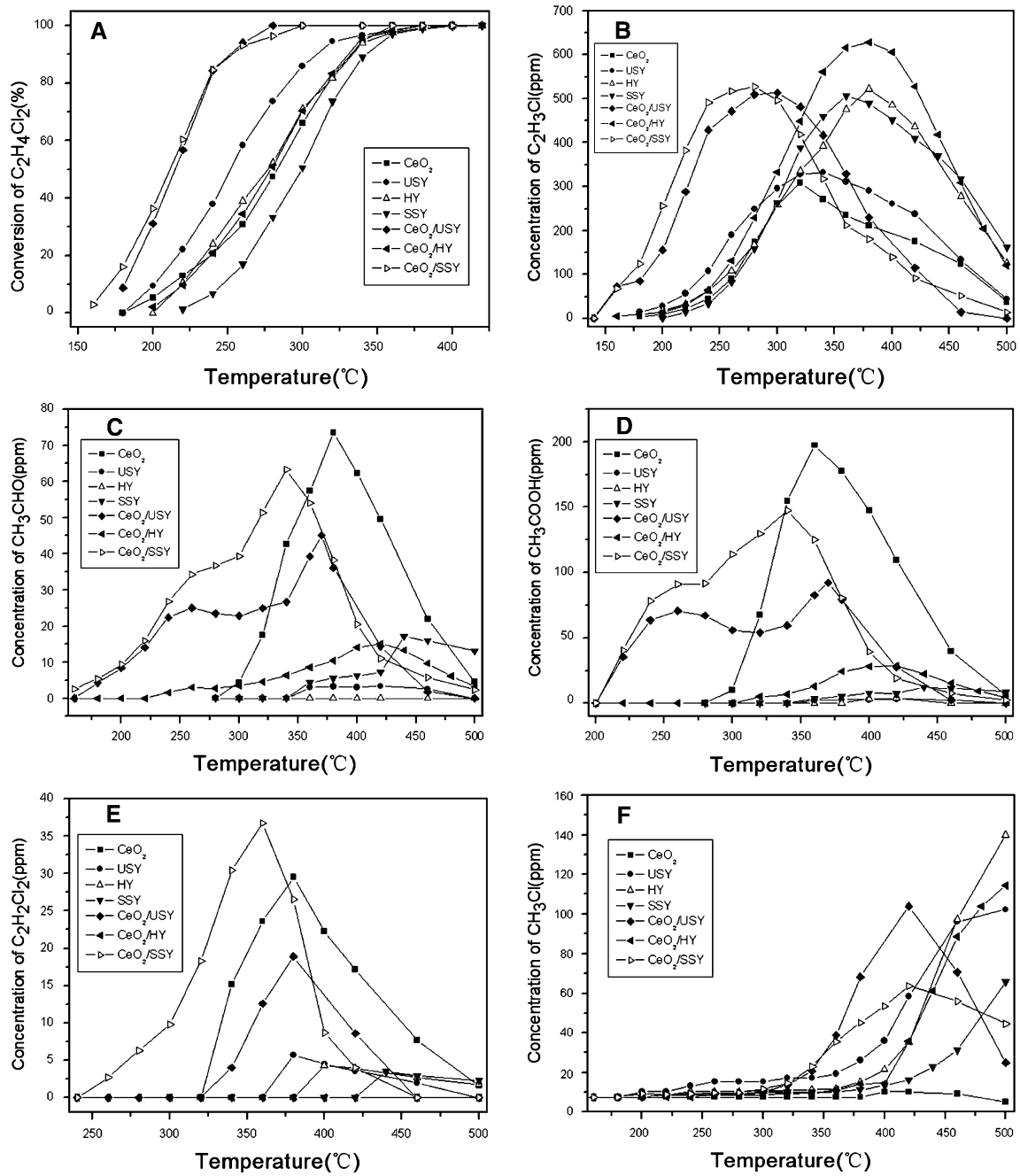

Fig. 1 The catalytic activity of CeO_2/Y catalysts. **a** conversion of $C_2H_4Cl_2$; **b** concentration of C_2H_3Cl; **c** concentration of CH_3CHO; **d** concentration of CH_3COOH; **e** concentration of $C_2H_2Cl_2$; **f** concentration of CH_3Cl

and three supports increases continuously until the reacting temperature reaches 500 °C. However, there is no CH_3Cl detected on CeO_2. As is known, there are strong acidic sites on Y zeolites, but not on CeO_2. So we suggest that there is a relationship between the acidity of catalysts and CH_3Cl. The stronger acidity there is on the catalysts, the easier for the catalysts to promote DCE cracking to CH_3Cl.

TPSR-MS method is used to follow the products of deep oxidation of DCE (shown in Fig. 2). Figure 2a–c shows the transformation of HCl, Cl_2, and CO_2 with temperature increasing on USY, CeO_2, and USY/CeO_2. Hydrogen chloride is the preferred chlorinated decomposition product instead of Cl_2, since it can be readily removed from the effluent stream by downstream aqueous scrubbing. From Fig. 2, it can be seen that HCl is the main product below 250 °C, the catalysts show a high selectivity (~100%) towards HCl formation. At higher than 400 °C, when conversion of DCE is complete, and

Table 2 C_{max} and T_{max} of different by-products on different catalysts

Catalyst	C_2H_3Cl		CH_3CHO		CH_3COOH		CH_3Cl		$C_2H_2Cl_2$	
	C_{max} (ppm)	T_{max} (°C)	C_{max} (ppm)	T_{max} (°C)	C_{max} (ppm)	T_{max} (°C)	C_{max} (ppm)	T_{max} (°C)	C_{max} (ppm)	T_{max} (°C)
CeO_2	310	320	74	380	198	360	10	420	30	380
USY	332	340	3.5	380	3.5	420	120	>500	6	380
HY	522	380	0	0	4	420	140	>500	4.3	400
SSY	508	360	17	365	13	440	69	>500	3.5	440
CeO_2/USY	513	300	25	260	71	260	104	420	19	380
			45	370	93	370				
CeO_2/HY	628	380	15	420	28	400	114	>500	0	0
CeO_2/SSY	529	280	34	260	91	260	64	420	37	360
			64	340	147	340				

chlorinated by-products are decomposed. Along with the reaction temperature increasing, HCl formation is mild. It is thought that the zeolite hydroxyls in the structure largely promoted HCl formation by the Deacon reaction [41]. Therefore, the acid character of the zeolites appears to be a favorable property to enhance HCl selectivity, mainly in the combustion of compounds with a low H/Cl ratio [42]. The relatively low Cl_2 selectivity of H-type zeolites indicates that the Deacon reaction occurs to a reduced extent over these catalysts. This is a desirable result taking into consideration that HCl is less toxic and can be easily trapped and neutralized from the effluent gas stream with a caustic solution. As far as CO_2 formation was concerned, there was observed a moderate selectivity to this deep oxidation product. Carbon dioxide clearly increase when the temperature reaches above 350 °C, which indicates that the deep oxidation of DCE is complete above 350 °C.

3.2 Catalyst Characterization

3.2.1 N_2 Adsorption/Desorption Results

The surface area data of these supports and catalysts are listed in Table 3. From Table 3 it can be seen that the surface area of CeO_2/Y catalysts decreases compared to that of those supports. Seen from the data, there is no relationship between catalytic activity and surface area.

3.2.2 XRD Results

Figure 3 shows the XRD patterns of Y-type zeolite and CeO_2/Y catalysts. The data of lattice parameters and crystallite size are listed in Table 4. From Fig. 3, it can be seen that the distinct fluorite-type oxide structure of CeO_2 are observed at about 28.6°, 33°, 47.6°, and 56.4 °. For all the CeO_2/Y catalysts, no characteristic peak of CeO_2 is observed, which suggests that CeO_2 is highly dispersed on the Y zeolites. After CeO_2 is loaded on Y zeolites, the intensity of Y zeolites, diffractive peaks is weaken and the lattice parameters increase, which indicates that some CeO_2 enter into the framework of Y zeolite. Interestingly at the opposite, the crystallite size of Y zeolite diminishes after CeO_2 is loaded. For CeO_2 particle of CeO_2/Y catalysts, the crystallite size changes but not the lattice parameters. The crystallite size of CeO_2 decreases in the order: CeO_2/SSY > CeO_2/USY > CeO_2 > CeO_2/HY, which evidently corresponds to their catalytic activity. As said above, we suggest that the catalytic decomposed reaction of DCE is sensitive to the framework of Y zeolites and crystallite size of CeO_2.

3.2.3 Temperature-Programmed Reduction (H_2-TPR) Results

Temperature-programmed reduction has been widely used to characterize oxygen-storage/release behavior of ceria-based materials. Cerium oxide is well known for its facile reducibility compared to other fluorite-type oxides [36]. Figure 4 shows the H_2-TPR profiles of CeO_2, CeO_2/USY, CeO_2/HY, and CeO_2/SSY. From Fig. 4, it can be seen that the there are three hydrogen consumption peaks during CeO_2 reduction in the range of 300–700 °C. The first two peaks at lower temperature (about 380 and 518 °C) are usually ascribed to the reduction of surface oxygen, and the third one at high temperature (>700 °C) is ascribed to the reduction of bulk oxygen of the CeO_2 structure [43]. No hydrogen consumption peaks are observed on USY, HY, and SSY supports (It is not lined out in Fig. 4). On CeO_2/HY there is only one peak at about 472 °C, but on CeO_2/USY and CeO_2/SSY, there are three peaks. The first two are for the reduction of surface oxygen of CeO_2 structure in the range of 300–600 °C. And the third one is for the reduction of bulk oxygen of the CeO_2 structure, which obviously decreases at about 670 and 709 °C. So the reduction performance of CeO_2 obviously changes in the

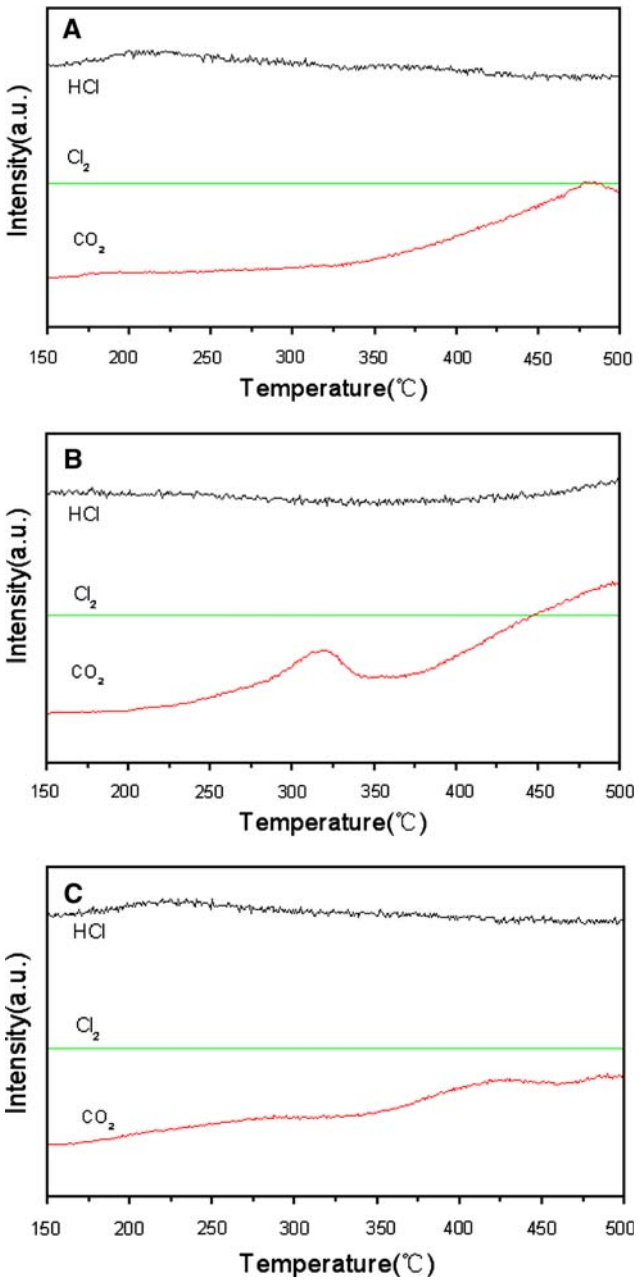

Fig. 2 TPSR-MS for the products of the oxidation of DCE over different catalysts: **a** products of DCE over USY; **b** products of DCE over CeO_2; **c** products of DCE over CeO_2/USY

Table 3 S_{BET} of different supports and catalysts

Catalysts	USY	HY	SSY	CeO_2	CeO_2/USY	CeO_2/HY	CeO_2/SSY
S_{BET} (m^2/g)	540.2	526.8	565.1	79.0	468.3	434.3	497.9

CeO_2/Y catalysts. The interaction between CeO_2 and Y zeolite is beneficial to the migration for bulk oxygen of the CeO_2 structure, which promotes the catalytic activity.

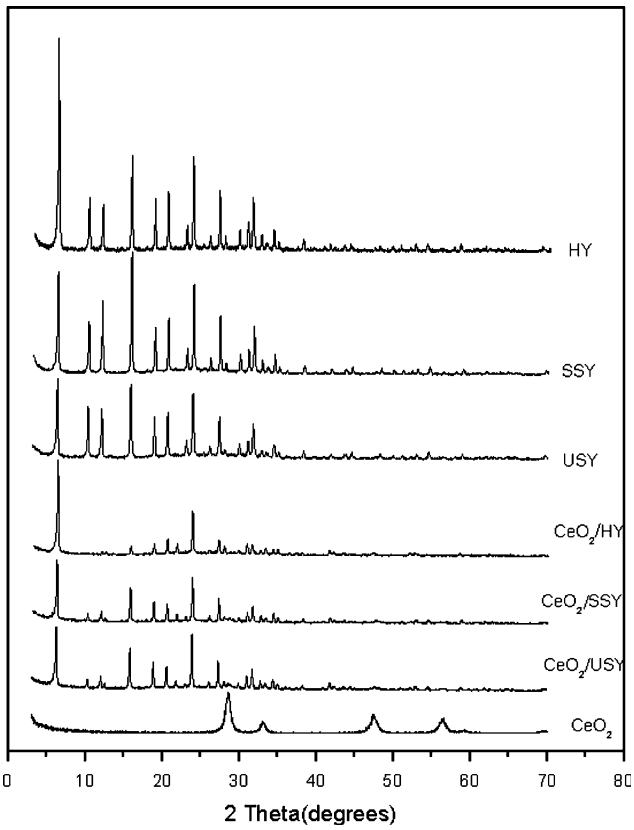

Fig. 3 XRD patterns of USY, HY, SSY, CeO_2, CeO_2/USY, CeO_2/HY, and CeO_2/SSY

3.2.4 NH_3-TPD Results

The acid properties of the catalytic materials were analyzed by TPD of ammonia. The NH_3-TPD profiles of the various catalysts investigated are shown in Fig. 5. The NH_3 described above 100 °C was considered as chemisorbed NH_3 and subsequently used for acidity determination. From the Fig. 5, it can been see that the total acidity which was the lowest of pure ceria. The Y zeolite supports and their CeO_2/Y catalysts have two major desorption peaks in 150–250 °C range. The much smaller desorption peaks were obtained in 300–450 °C range indicating the presence of strong Brønsted acid sites. On the contrary, CeO_2 showed almost no inflection in this region. Additionally, the TPD profiles also evidenced the presence of acid sites of different strength on each sample. The amount of ammonia desorbing above a certain temperature was taken as the acid sites concentration and the peak desorption temperatures of the TPD profile were assumed to be measures of the relative strength of the sites. In an attempt to characterize the acid strength sites retaining NH_3 at temperatures higher than 300 °C were considered as strong sites, and accordingly the sites retaining NH_3 at temperatures lower than 300 °C were considered as weak acid sites [38].

Table 4 XRD patterns of different supports and catalysts

Catalysts	Lattice parameters of Y zeolite (nm)	Crystallite size of Y zeolite (nm)	Lattice parameters of CeO_2 (nm)	Crystallite size of CeO_2 (nm)
USY	24.48944	53.7	–	–
HY	24.64311	74.3	–	–
SSY	24.46676	70.7	–	–
CeO_2	–	–	5.40822	10.3
CeO_2/USY	24.51076	50.7	5.39848	11.7
CeO_2/HY	24.65695	71.7	5.41165	9.6
CeO_2/SSY	24.51126	68.1	5.39948	12.4

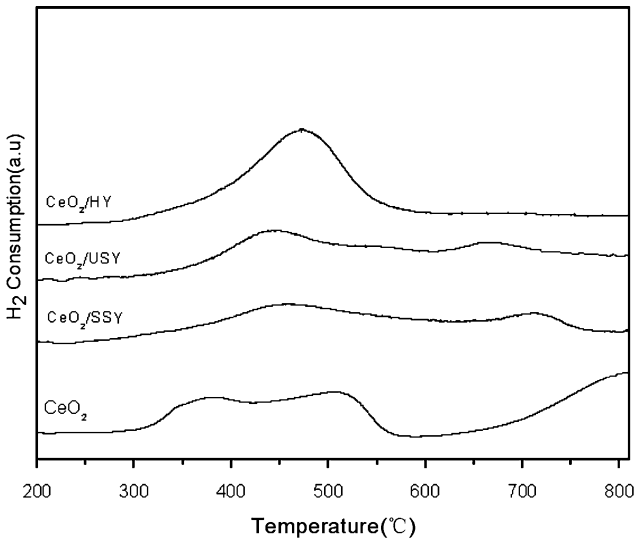

Fig. 4 TPR profiles of the Y zeolites catalysts

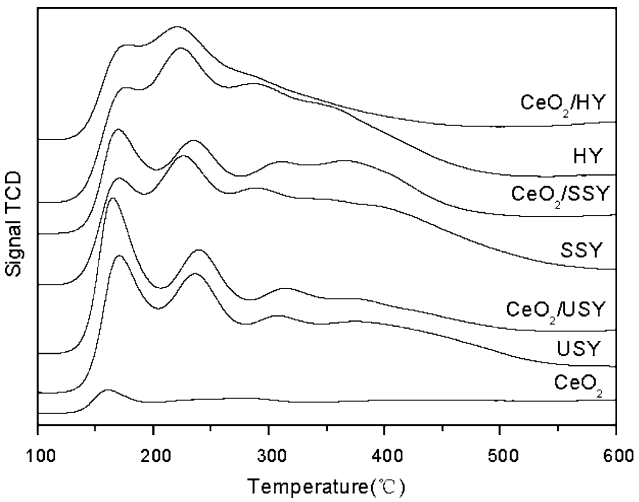

Fig. 5 NH_3-TPD profiles of the Y zeolites catalysts

4 Conclusion

The purpose of this work is to evaluate the catalytic activity of a series of CeO_2/Y catalysts for deep oxidation of DCE at lean concentration conditions (about 1,000 ppm) between 160 and 500 °C. The supports and catalysts are characterized by XRD, N_2 adsorption/desorption, and H_2-TPR. The catalytic reaction results indicate that: CeO_2/USY and CeO_2/SSY are the most active catalysts, $T_{98\%}$ values of which are about 270 and 290 °C, respectively. The catalytic oxidation of DCE occurs at relative low temperature. However, with this rapid decomposition, the main intermediate C_2H_3Cl is produced. C_2H_3Cl can be completely decomposed to CO_2 and HCl at higher temperature. On CeO_2/USY and CeO_2/SSY, the peak temperature at which the maximum concentration of C_2H_3Cl appears are lower, at about 300 and 280 °C, respectively. It shows that there is higher dehydrochlorination performance on CeO_2/USY and CeO_2/SSY during catalytic destruction of DCE. Characterization results indicate that the interaction between CeO_2 and Y zeolite directly affects the catalytic activity of CeO_2/Y catalysts. XRD analysis indicates that CeO_2 is highly dispersed on the Y zeolite supports. The changes of lattice parameters and crystallite size of Y zeolite and CeO_2 on CeO_2/Y catalysts directly affect the catalytic activity of deep oxidation of DCE. TPR analysis indicates that the interaction between CeO_2 and Y zeolite is beneficial to the migration of bulk oxygen of the CeO_2 structure, which can promote the catalytic activity of CeO_2/Y.

Acknowledgments We gratefully acknowledge the financial supports from the Ministry of Science and Technology of China (No. 2004 CB 719504) and Nature Science Foundation of China (No. 20577043).

References

1. Moretti EC (2001) Practical solutions for reducing volatile organic compounds and hazardous air pollutants. Center for Waste Reduction Technologies of the American Institute of Chemical Engineers, New York
2. López-Fonseca R, de Rivas B, Gutiérrez-Ortiz JI, Aranzabal A, González-Velasco JR (2003) Appl Catal B 41:31
3. Hunter P, Oyama ST (2000) Control of volatile organic compound emissions: conventional and emerging technologies. Wiley-Interscience, New York

4. Mendyka B, Musialik-Piotrowska A, Syczewska K (1992) Catal Today 11:597
5. Imamura S (1992) Catal Today 11:547
6. Krishnamoorthy S, Rivas JA, Amiridis MD (2000) J Catal 193:264
7. Agarwal SK, Spivey JJ, Butt JB (1992) Appl Catal A 81:239
8. Chatterjee S, Greene HL, Park YJ (1992) J Catal 138:179
9. Rachapudi R, Chintawar PS, Greene HL (1999) J Catal 185:58
10. Jeong K-E, Kim D-C, Ihm S-K (2003) Catal Today 87:29
11. Spivey JJ, Butt JB (1992) Catal Today 11:465
12. Chen NY, Degnan TF Chem Eng Prog (1998) 32
13. Corma A, Martínez A (1993) Catal Rev-Sci Eng 35:483
14. Ruthven DM (1988) Chem Eng Prog 84:43
15. Imamura S, Tarumoto H, Ishida S (1989) Ind Eng Chem Res 28:1449
16. Chatterjee S, Greene HL (1991) J Catal 130:76
17. Karmakar S, Greene HL (1992) J Catal 138:364
18. González-Velasco JR, López-Fonseca R, Aranzabal A, Gutiérrez-Ortiz JI, Steltenpohl P (2000) Appl Catal B 24:233
19. López-Fonseca R, Aranzabal A, Gutiérrez-Ortiz JI, Álvarez-Uriarte JI, González-Velasco JR (2001) Appl Catal B 30:303
20. Corma A, Garcia H, Iborra S, Primo J (1989) J Catal 120:78
21. Zimmer P, Tschöpe A, Birringer R (2002) J Catal 205:339
22. Skårman B, Grandjean D, Benfield RE, Hinz A, Andersson A, Wallenberg LR (2002) J Catal 211:119
23. Liu YY, Hayakawa T, Suzuki K, Hamakawa S, Tsunoda T, Ishii T, Kumagai M (2002) Appl Catal A 223:137
24. Tang XL, Zhang BC, Li Y, Xu YD, Xin Q, Shen WJ (2004) Catal Today 93:19
25. Sayle XT, Parkerb SC, Sayle DC (2005) Phys Chem Chem Phys 7:2936
26. Liu W, Flytzani-Stephanopoulos M (1995) J Catal 153:304
27. Knauth P, Schwitzgebel G, Tschöpe A, Villain S (1998) J Solid State Chem 140:295
28. Imamura S, Fukuda I, Ishida S (1988) Ind Eng Chem Res 27:718
29. Mishra VS, Mahajani VV, Joshi JB (1995) Ind Eng Chem Res 34:2
30. Lin SS, Chen CL, Chang DJ, Chen CC (2002) Water Res 36:3009
31. Lin SS, Chang DJ, Wang CH, Chen CC (2003) Water Res 37:793
32. Wang CH, Lin SS (2004) Appl Catal A 268:227
33. Dai QG, Wang XY, Lu GZ (2007) Catal Commun 8:1645
34. López-Fonseca R, Aranzabal A, Steltenpohl P, Gutiérrez-Ortiz JI, González-Velasco JR (2000) Catal Today 62:367
35. de Rivas B, L′opez-Fonseca R, Gonz′alez-Velasco JR, Guti′errez-Ortiz JI (2007) J Mol Catal A Chem 278:181
36. Gutiérrez-Ortiz JI, de Rivas B, López-Fonseca R, González-Velasco JR (2004) Appl Catal A 269:147
37. de Rivas B, Gutie′rrez-Ortiz JI, Lo′pez-Fonseca R, Gonza′lez-Velasco JR (2006) Appl Catal A 314:54
38. Gutie′rrez-Ortiz JI, de Rivas B, Lo′pez-Fonseca R, Gonza′lez-Velasco JR (2006) Appl Catal B 65:191
39. Gutie′rrez-Ortiz JI, de Rivas B, Lo′pez-Fonseca R, Gonza′lez-Velasco JR (2005) Catal Today 107–108:933
40. Ramanathan K, Spivey JJ (1989) Combust Sci Technol 63:247
41. Ramachandran B, Greene HL, Chatterjee S (1996) Appl Catal B 8:157
42. López-Fonseca R, Gutiérrez-Ortiz JI, Gutiérrez-Ortiz MA, González-Velasco JR (2002) J Catal 209:145
43. Bigey C, Hilaire L, Maire G (2001) J. Catal 198:208